بسم الله الرحمن الرحيم

www.aecenar.com/institutes/iap

IAP-IRS

Infrared Astronomy Measurement System

1st Project Report (2018)

- Basics
- Concept for Instrument

Initial document: Ras Masqa/Tripoli, 06 November 2018

Last update: 28.06.2019

Authors:

Dr. Samir Mourad

Content

Project Status at Beginning of actual project phase

بسم الله الرحمن الرحيم

AECENAR
Association for Economical and Technological Cooperation in the Euro-Asian and North-African Region
www.aecenar.com

IAP INSTITUTE FOR ASTROPHYSICS

Ras Masqa/Tripoli, Lebanon 06-11-2018

Infrared Sensor System for IAP-SAT (IAP-IRS)

The IAP project aims to investigate a proper low cost platform to take insterstellar data in IR and radio spectrum. There are the following working packages for 2018-2020:

- Detailed space infrared sensor
- Detailed Mission Planning for bringing IAP-SAT into orbit
- Collect data from IAP-SAT

Illustration 1 : Caption: Black Widow nebula captured by Spitzer's IRAC. Credit: NASA/JPL-Caltech/E. Churchwell (University of Wisconsin-Madison) and the GLIMPSE Team

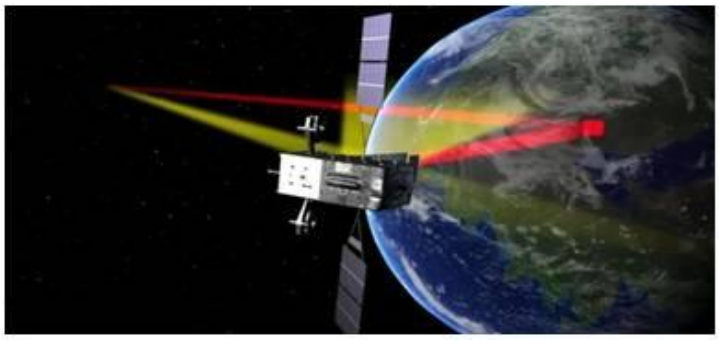

Illustration 2: The Space Based Infrared System can spot heat causing events across the world

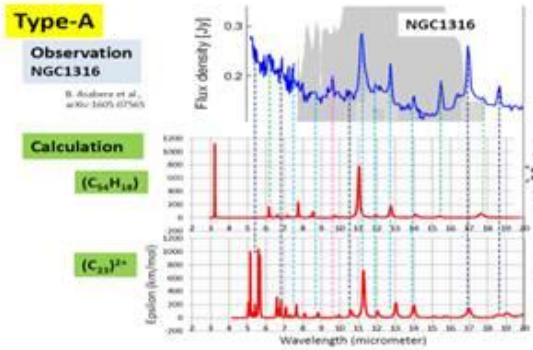

Illustration 3: Type-A spectrum. Calculated spectrum of (C54H18) and $(C23)^{2+}$ are compared with observed one of NGC1316. Blue dashed lines coincident with both molecules, whereas green with only (C54H18), black with $(C23)^{2+}$, pink no coincidence with both molecules.

Tasks:

- Design of a proper infrared sensor.
- Collect IR data from satellite platform in Canopus Region.

Contact:

Dr. Samir Mourad,
Mob./WhatsApp +961 76 341526
Email: samir.mourad@aecenar.com

1 Project Management

1.1 Organisation within IAP

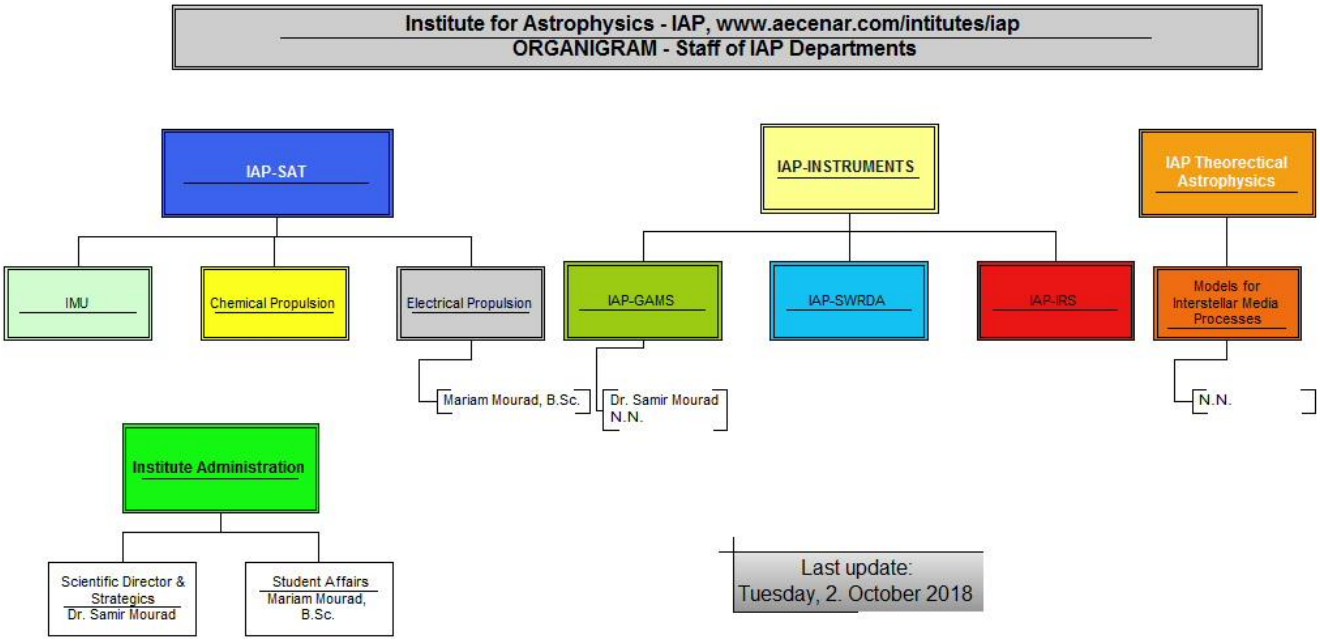

1.2 Working Packages and Time Plan

1.2.1 To do with internal ressources

WP No.	Working package content	Time span, costs	Development environment (HW, SW)	Responsible	Status

1.2.2 To do with external ressources

WP No.	Working package content	Time span, costs	Development environment (HW, SW)	Responsible	Status

2 Basics

2.1 Infrared (Near Infrared, Mid Infrared, Far Infrared)[1]

Infrared is usually divided into 3 spectral regions: near, mid and far-infrared. The boundaries between the near, mid and far-infrared regions are not agreed upon and can vary. The main factor that determines which wavelengths are included in each of these three infrared regions is the type of detector technology used for gathering infrared light.

Near-infrared observations have been made from ground based observatories since the 1960's. They are done in much the same way as visiblelight observations for wavelengths less than 1 micron, but require special infrared detectors beyond 1 micron. Mid and far-infrared observations can only be made by observatories which can get above our atmosphere. These observations require the use of special cooled detectors containing crystals like germanium whose electrical resistance is very sensitive to heat.

Infrared radiation is emitted by any object that has a temperature (i.e. radiates heat). So, basically all celestial objects emit some infrared. The wavelength at which an object radiates most intensely depends on its temperature. In general, as the temperature of an object cools, it shows up more prominently at farther infrared wavelengths. This means that some infrared wavelengths are better suited for studying certain objects than others.

Visible (courtesy of Howard McCallon), near-infrared (2MASS), and mid-infrared (ISO) view of the Horsehead Nebula. Image assembled by Robert Hurt.

As we move from the near-infrared into mid and far-infrared regions of the spectrum, some celestial objects will appear while others will disappear from view. For example, in the above image you can see how more stars (generally cooler stars) appear as we go from the visible light image to the near-infrared image. In the near-infrared, the dust also becomes transparent, allowing us to see regions

[1] http://www.icc.dur.ac.uk/~tt/Lectures/Galaxies/Images/Infrared/Regions/irregions.html

hidden by dust in the visible image. As we go to the mid-infrared image, the cooler dust itself glows. The table below highlights what we see in the different infrared spectral regions.

SPECTRAL REGION	WAVELENGTH RANGE (microns)	TEMPERATURE RANGE (degrees Kelvin)	WHAT WE SEE
Near-Infrared	**(0.7-1) to 5**	**740 to (3,000-5,200)**	**Cooler red stars Red giants Dust is transparent**
Mid-Infrared	**5 to (25-40)**	**(92.5-140) to 740**	**Planets, comets and asteroids Dust warmed by starlight Protoplanetary disks**
Far-Infrared	**(25-40) to (200-350)**	**(10.6-18.5) to (92.5-140)**	**Emission from cold dust Central regions of galaxies Very cold molecular clouds**

2.1.1 NEAR INFRARED:

As we move away from visiblelight towards longer wavelengths oflight, we enter the infrared region. As we enter the near-infrared region, the hot blue stars seen clearly in visible light fade out and cooler stars come into view. Large red giant stars and low mass red dwarfs dominate in the near-infrared. The near-infrared is also the region where interstellar dust is the most transparent to infrared light.

Visible (left) and Near-Infrared View of the Galactic Center
Visible image courtesy of Howard McCallon. The infrared image is from the 2 Micron All Sky Survey (2MASS)

Notice in the above images how center of our galaxy, which is hidden by thick dust in visible light (left), becomes transparent in the near-infrared (right). Many of the hotter stars in the visible image have faded in the near-infrared image. The near-infrared image shows cooler, reddish stars which do not appear in the visible light view. These stars are primarily red dwarfs and red giants.

Red giants are large reddish or orange stars which are running out of their nuclear fuel. They can swell up to 100 times their original size and have temperatures which range from 2000 to 3500 K. Red giants radiate most intensely in the near-infrared region.

Red dwarfs are the most common of all stars. They are much smaller than our Sun and are the coolest of the stars having a temperature of about 3000 K which means that these stars radiate most strongly in the near-infrared. Many of these stars are too faint in visiblelight to even be detected by optical telescopes, and have been discovered for the first time in the near-infrared.

2.1.2 MID INFRARED:

As we enter the mid-infrared region of the spectrum, the cool stars begin to fade out and cooler objects such as planets, comets and asteroids come into view. Planets absorb light from the sun and heat up. They then re-radiate this heat as infrared light. This is different from the visible light that we see from the planets which is reflected sunlight. The planets in our solar system have temperatures ranging from about 53 to 573 degrees Kelvin. Objects in this temperature range emit most of their light in the mid-infrared. For example, the Earth itself radiates most strongly at about 10 microns. Asteroids also emit most of their light in the mid-infrared making this wavelength band the most efficient for locating dark asteroids. Infrared data can help to determine the surface composition, and diameter of asteroids.

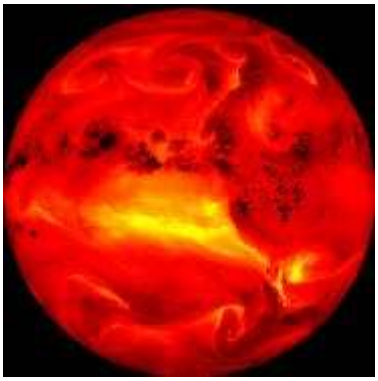

An infrared view of the Earth

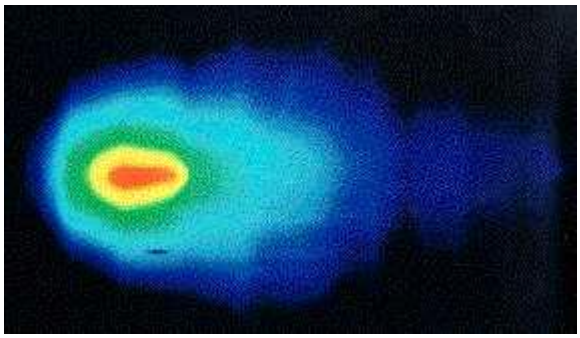

IRAS mid-infrared view of Comet IRAS-Araki-Alcock

Dust warmed by starlight is also very prominent in the mid-infrared. An example is the zodiacal dust which lies in the plane of our solar system. This dust is made up of silicates (like the rocks on Earth) and range in size from a tenth of a micron up to the size of large rocks. Silicates emit most of their radiation at about 10 microns. Mapping the distribution of this dust can provide clues about the formation of our own solar system. The dust from comets also has strong emission in the mid-infrared.

Warm interstellar dust also starts to shine as we enter the mid-infrared region. The dust around stars which have ejected material shines most brightly in the mid-infrared. Sometimes this dust is so thick that the star hardly shines through at all and can only be detected in the infrared. Protoplanetary disks, the disks of material which

surround newly forming stars, also shines brightly in the mid-infrared. These disks are where new planets are possibly being formed.

2.1.3 FAR INFRARED:

In the far-infrared, the stars have all vanished. Instead we now see very cold matter (140 Kelvin or less). Huge, cold clouds of gas and dust in our own galaxy, as well as in nearby galaxies, glow in far-infrared light. In some of these clouds, new stars are just beginning to form. Far-infrared observations can detect these protostars long before they "turn on" visibly by sensing the heat they radiate as they contract."

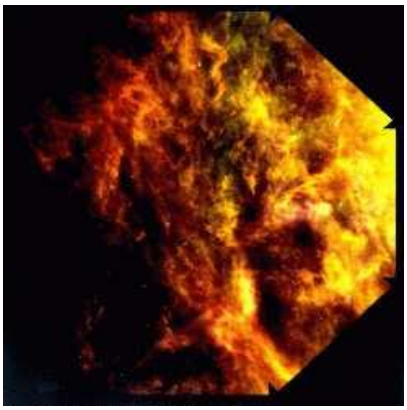

IRAS view of infrared cirrus - dust heated by starlight

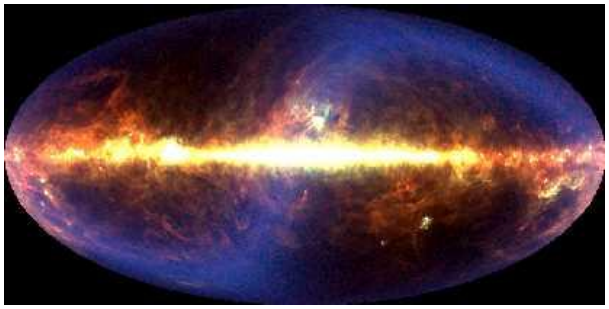

Michael Hauser (Space Telescope Science Institute),
the COBE/DIRBE Science Team, and NASA

The center of our galaxy also shines brightly in the far-infrared because of the thick concentration of stars embedded in dense clouds of dust. These stars heat up the dust and cause it to glow brightly in the infrared. The image (at left) of our galaxy taken by the COBE satellite, is a composite of far-infrared wavelengths of 60, 100, and 240 microns.

Except for the plane of our own Galaxy, the brightest far-infrared object in thesky is central region of a galaxy called M82. The nucleus of M82 radiates as much energy in the far-infrared as all of the stars in our Galaxy combined. This far-infrared energy comes from dust heated by a source that is hidden from view. The central regions of most galaxies shine very brightly in the far-infrared. Several galaxies have active nuclei hidden in dense regions of dust. Others, called starburst galaxies, have an extremely high number of newly forming stars heating interstellar dust clouds. These galaxies, far outshine all others galaxies in the far-infrared.

IRAS infrared view of the Andromeda Galaxy (M31) - notice the bright central region.

2.2 Definition of infrared and the origin of the infrared radiation[2]

Table of Contents

[2] http://elte.prompt.hu/sites/default/files/tananyagok/InfraredAstronomy/ch03.html

In this chapter we describe the technological and observational justification of the infrared band. Atomic and molecular transitions are investigated as the origin of the infrared radiation.

Electromagnetic radiation is classified by wavelength into gamma rays, X-rays, ultraviolet, visible, infrared, microwave and radio, see on Figure 3.1. Infrared radiation lies between the visible and microwave part of the electromagnetic radiation.

2.2.1 The definition of the infrared band

The quantum efficiency is a measure of a device's electrical sensitivity to light. It is the incident photon to converted electron ratio, i.e. the percentage of photons hitting the device's photoreactive surface that produce charge carriers. It is measured in electrons per photon or amps per watt. As we see in Figure 3.1 the quantum efficiency of the human eye is around 1% to 10%, over most conditions (see eg. http://psych.nyu.edu/pelli/pubs/pelli1990efficiency.pdf). It gets slightly better for red colour at low light levels (photopic vision), but our eyes lose all sensitivity beyond the red end of the visible spectrum ($\lambda > 0.75$ μm).

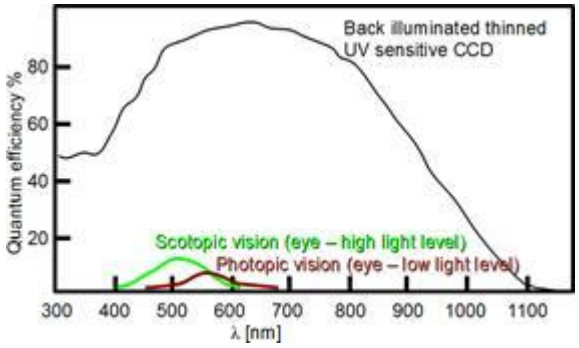

Figure 3.1: *Quantum efficiency of human eye and CCD*

The infrared quantum efficiency of typical photoemulsions is similar to the human eye, however infrared sensitive astrographic photo plates (Kodak IVN) were sensitive up to $\lambda \approx 1$ μm. We can not use any more most of the visible band technologies such as photography, CCDs and photocathodes for $\lambda > 1.1$ μm, and that wavelength limit can be considered as a technical border of infrared at the short wavelength side. Referring to Figure 3.1 we note that the CCD surface has channels used for charge transfer that are shielded by polysilicon gate electrodes which absorb light (mostly blue). Such losses are eliminated in the back-illuminated CCD, where the light falls onto the back of the CCD in a region that has been thinned so it is transparent. The wavelength dependent specific detectivity D^* is defined as reciprocal of noise-equivalent power (NEP), normalized per unit area:

$$D^* = \frac{\sqrt{\text{Area}}}{\text{NEP}}, \tag{3.1}$$

where Area is the photosensitive region of the detector. The unit of D^* is: $cmHz^{½}W^{-1}$.

Figure 3.1 shows the specific detectivity D of the most common compounds used as detectors which include:

Gallium Arsenide – GaAs, Lead Sulfide – PbS, Indium Antimonide – InSb, Germanium doped with Copper - Ge:Cu, Germanium doped with Zinc - Ge:Zn, Germanium doped with Gold - Ge:Au, Germanium doped with Gallium - Ge:Ga, Lead Telluride – PbTe, phosphorus-doped silicon – Si:P.

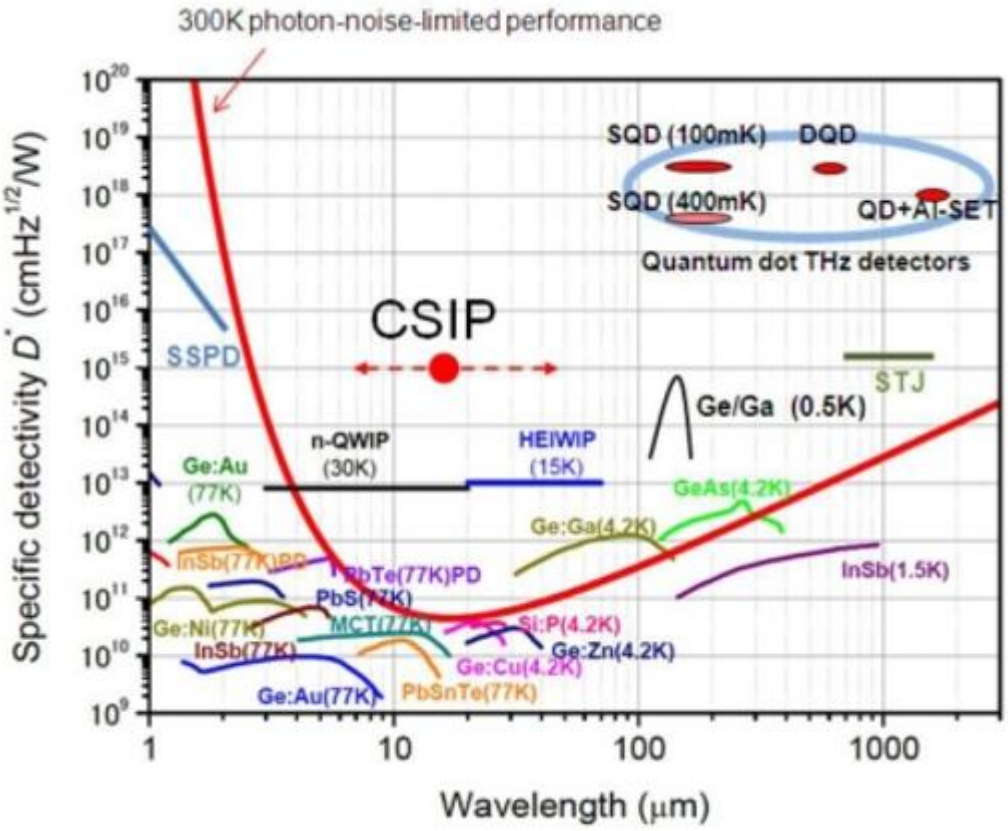

Figure 3.2: Spectral response characteristics of various infrared detectors. (Ueda T, Komiyama S, 2010, http://openi.nlm.nih.gov/detailedresult.php?img=3231243_sensors-10-08411f7&req=4)

The highest available frequency band of terrestrial sub-mm observatories is at 810GHz (0.37mm). The ”end” of the infrared region is again technologically defined: it is the wavelength (≈ 350μm) where radio techniques such as superheterodyne receivers tend to be used in preference to the ”optical style” infrared approach and the incoming radiation tends to be thought of as waves rather than individual photons. The region from 0.35mm to 1mm is referred to as the sub-millimeter region. It may be regarded as a subdivision of radio astronomy.

Astronomical justification for the definition is that already at 2.2μm the sky has a significantly different appearance from the visible one. The cooler end of the stellar population becomes predominant and some objects turn out to have infrared fluxes much higher than predicted from their visible spectra.

These infrared excesses can be due to cool dust shells surrounding them or to circumstellar free-free emission for example. The most important sources of the infrared photons are Solar system objects, stars and extended galactic objects, extragalaxies. The cosmic microwave background (CMB) is the relic of the Big Bang. It is characterized by a blackbody spectrum of temperature 2.73K. The rise of its spectrum marks the end of the infrared.

The vibrational transitions of molecules results infrared photons, whereas we observe their rotational transitions spectra in the sub-mm and radio region.

Infrared is divided into three parts: near, mid and far-infrared. Near-infrared refers to the part of the infrared spectrum that is closest to visible light and far-infrared refers to the part that is closer to the microwave region. Mid-infrared is the region between these two. The boundaries between these regions are not exact and can vary. (Table 3.1. shows the general properties of the infrared ranges.)

Infrared radiation	Wavelength range [μm]	Astronomical objects
Near	1-5	Red giants Cooler red stars
Mid	5-30	Planets, comets and asteroids Protoplanetary disks
Far	30-400	Central regions of galaxies Emission from cold dust

Table 3.1: *Properties of the infrared ranges*

A justification based on the observational conditions can be made as well. Beyond 2.3μm blackbody radiation from the telescope and the atmosphere itself begins to dominate other sources of background. Measurements of faint astronomical objects have to be made by alternatively observing the field containing the source and a nearby ”empty” one. This process is known as chopping. The signals are subtracted to eliminate the strong background. Alternatively the measurement is taken outside the atmosphere with a cooled observing system.

In the NIR, MIR and FIR the main sources of the background are terrestrial, Zodiacal light and galactic ISM radiation. From about 300μm CMB starts to dominate the background. Except bands in the NIR, the infrared sky is to be observed by air-borne or space-borne instruments.

The sub-millimeter region however can be accessed again in selected atmospheric windows by terrestrial telescopes located at high altitude, low precipitable water vapor (pwv) sites like Mauna Kea or South Pole. Precipitable water is the measure of the depth of liquid water at the surface that would result after precipitating all of the water vapor in a vertical column over a given location, usually extending from the surface to 300 mb (http://forecast.weather.gov/glossary.php?word=precipitable%20water).

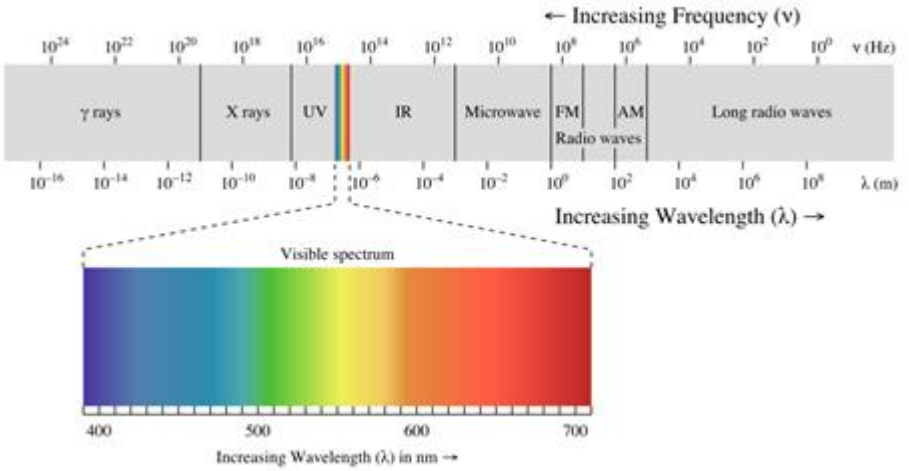

Figure 3.3: Electromagnetic spectrum (http://en.wikipedia.org/wiki/File:EM_spectrum.svg) from 10^{-16} to 10^{8} m. The visible spectrum located in the middle, it covers only a small part of the spectrum.

Observations at different wavelengths reveal various pictures from astronomical objects. Figure 3.4 shows the M51 Spiral Galaxy at different wavelengths: from visible to far infrared. Observations of visible light show the stars that make up the galaxy. Infrared observations reveal the mixture of gas and dust from which new stars can be born.

Figure 3.4: Hubble, 2MASS, Spitzer Space Telescope, ISO and IRAS observations of M51 Spiral Galaxy. Shorter wavelengths show the star content of it, on longer wavelengths the radiation of gas and dust dominate. (http://astromic.blogspot.de/2011/02/infrared-astronomy.html)

Near-infrared observations have been made from ground based observatories since the 1960's. This part of the infrared radiation can be observed with similar technique as visible light, but it requires special infrared detectors. Mid and far-infrared observations, where the wavelength is longer than 20 μm, can only be made by observatories which can get above our atmosphere. These observations require the use of special cooled detectors.

2.3 Instrumentation / Sensors Technology

2.3.1 IRAS

The Infrared Astronomical Satellite (IRAS) was initiated in 1975, designed and constructed by NASA (USA), NIVR (the Netherlands), and SERC (UK), and launched by NASA (launcher: Delta 3910) on January 25, 1983. It was the first space-borne infrared observatory to scan the entire sky. During its ten months of operation, IRAS scanned more than 96 percent of the sky four times at four infrared bands centered at 12, 25, 60 and 100 microns. Its main task was to discover and measure IR point sources. The IRAS mission has had a major impact on almost every area of astronomy.

2.3.1.1 The most important results of IRAS:

- Detected about 350,000 infrared sources (see Figure 6.1), increasing the number of cataloged astronomical sources by about 70%.

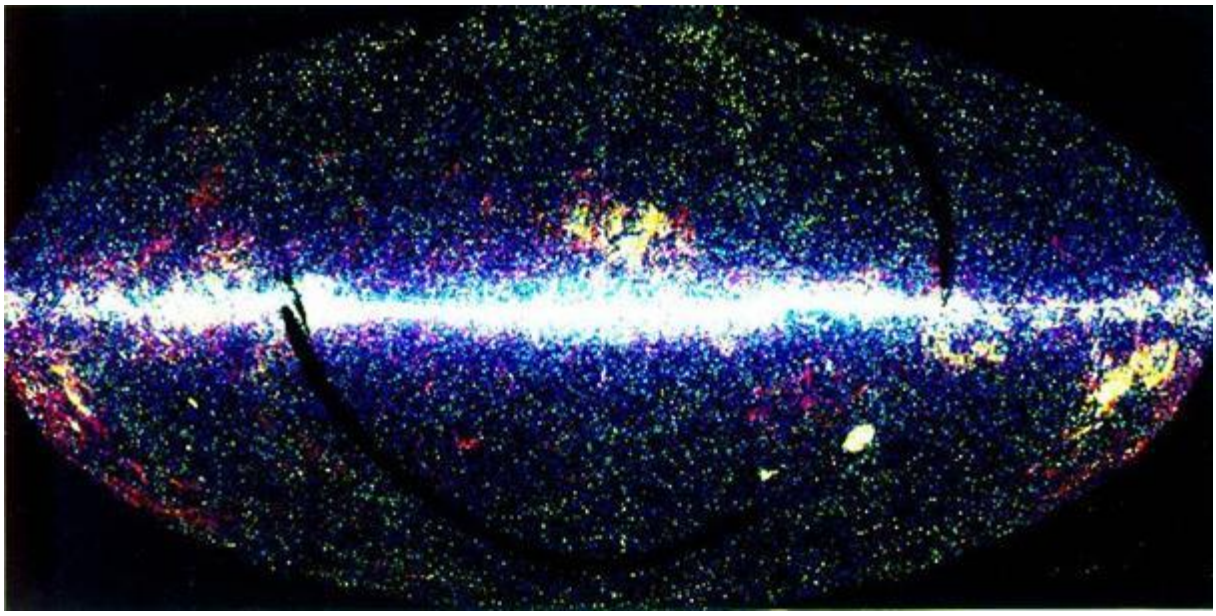

Figure 6.1: *All sky map of IRAS sources (*http://www.iras.ucalgary.ca/~nkoning/irasDb/iras.html*)*

- Discovered 6 new comets
- Found that comets are dustier than previously thought and that dust from comets fills the Solar System
- Detected useful infrared data for 2004 asteroids
- Detected the zodiacal dust bands - bands of infrared emission that girdle our solar system which are likely to be debris from asteroid collisions
- Found evidence of zodiacal dust bands around other stars
- Discovered a disk of dust grains around the star Vega, see Figure 6.2. The significant excess above the photospheric model indicates the presence of cold material around a star.

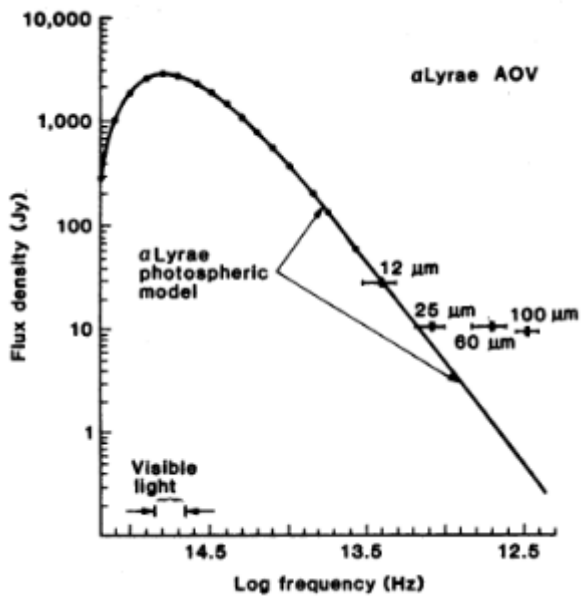

Figure 6.2: *Observed spectral enery distribution of Vega and photosperic stellar model (Neugebauer et al.).*

- Detected disks of material around several other stars.
- Detected several probable protostars embedded in clouds of gas and dust
- Found that some Bok globules contain protostars. e.g. Beichman (1984) showd that the Bok globule, Barnard 5 contains at least four protostars.
- Cataloged thousands of hot, dense cores within clouds of gas and dust which could be newly forming stars
- Cataloged over 12,000 variable stars, the largest collection known to date
- Revealed for the first time the core of our galaxy
- Found infrared cirrus (wisps of warm dust) in almost every direction of space
- Data from IRAS was used to show that our galaxy is a barred spiral galaxy - a galaxy which has an elongated central bar-like bulge from which its spiral arms unwind.
- Detected 75,000 starburst galaxies - galaxies which are extremely bright in the infrared due to intense star formation. It was found that many of these starburst galaxies have ”superwinds” emerging from their centers due to the large number of supernova explosions which occur in these galaxies.
- Detected strong infrared emission from interacting galaxies
- First identified IRAS F10214+4724 - at the time, the most luminous object known in the Universe by a factor of 2. This object may be the best candidate for a forming spiral galaxy yet discovered.

2.3.1.2 Instruments and observing strategy of IRAS

IRAS telescope system comprised the upper part of the satellite and was composed of a two mirror, Ritchey-Chretien telescope mounted within a toroidal superfluid helium tank, which in turn was mounted within the evacuated main shell. The optical system was protected from contamination before launch and during the first week of the mission by an aperture

cover cooled with supercritical helium. After the cover was ejected, the sunshade limited heat flow to the aperture by blocking direct solar radiation and reflecting away terrestrial infrared radiation. The telescope orientation was constrained to prevent sunlight from striking the inner surface of the sunshade and radiation from the Earth from illuminating the radiators around the telescope aperture. The telescope was cooled by contact with the superfluid helium tank to temperatures ranging from 2 to 5 K. The surfaces of the sunshade which could be viewed by the telescope aperture were cooled by a three-stage radiator to about 95 K.

The focal plane assembly contained the infrared and visible detectors, cold electronics, and associated masks, filters and field optics. It consisted of 62 infrared channels and eight visible channels. The infrared channels were divided into eight modules, two for each color band with each module containing either seven or eight detectors. The detector masks were rectangular in aspect and infrared sources scanned across the focal plane parallel to the narrow dimension of the detectors in all observational modes.

2.4 Infrared satellite observatories

Table of Contents

In this chapter we give an overview of the observing strategy, scientific instruments and main scientific result of Infrared Space Observatory, Spitzer Space Telescope and Herschel Space observatory.

2.4.1 Infrared Space Observatory (ISO)

ISO observed the infrared sky between February 1996 and April 1998. It was a European Space Agency (ESA) mission, launched in November 1995. The satellite weighed around 2500 kg and was launched with over 2000 litre of liquid helium coolant on board, which lasted for 29 months.

ISO was the first orbiting infrared observatory. It made during its lifetime more than 30 000 individual observations of all kind of astronomical objects: in the solar system and in the most distant galaxies.

The telescope operated between 2.5 and 240 μm. Comparing to IRAS, at 12 μm it was one thousand times more sensitive and had one hundred times better angular resolution.

Figure 7.1 shows ISO's two largely independent modules: the Payload Module and the Service Module. The Payload Module was a large cryostat containing super fluid helium which maintained the telescope and the scientific instruments at temperatures between 2 and 8 K. The Service Module contained the warm electronics of the scientific instruments and all the classical spacecraft subsystems, which are necessary to supply the basic functions. The sun-shield with solar cells always faced the Sun to provide electrical power and to protect the Payload Module from direct irradiation.

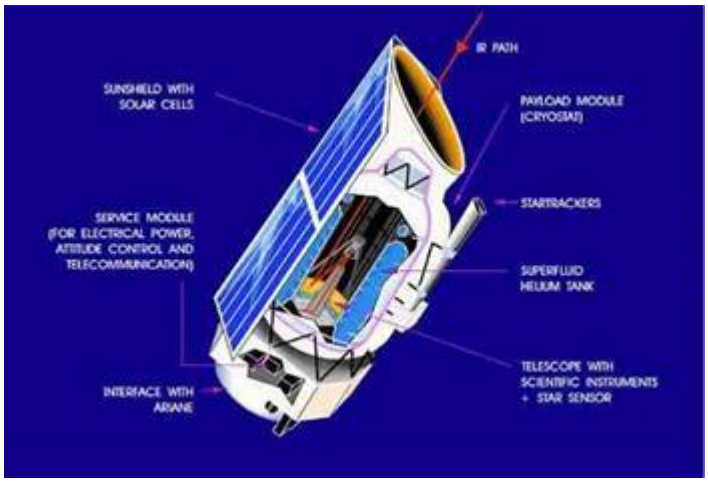

Figure 7.1: Schematic view of the ISO satellite, two largely independent modules are visible: the Payload Module and the Service Module

http://vietsciences.free.fr/giaokhoa/vatly/thienvan/gsnguyenquangrieu/images/iso_satellite.jpg

The ISO telescope was a 60 cm diameter Richey-Chrétien system with an overall focal ratio of f/15. This type of telescope is free from coma and spherical aberration, and they have larger field of view than the classical Cassegrain type telscopes. The optical quality of the primary and secondary mirrors provided diffraction limited performance at wavelengths beyond 5 μm, also limited by pointing performance.

ISO had a high Earth orbit with a period of one-to-two days. It was accustomed by previous space observatories.

2.4.1.1 Scientific instruments and observing strategy

ISO's four scientific instruments are the following: a camera, ISOCAM, an imaging photo-polarimeter, ISOPHOT, and the two spectrometers, a long wavelength LWS and a short wavelength SWS.

The telescope and the scientific instruments operated at ~3K. Some of the infrared detectors were cooled down to 1.8 K. This low temperature enabled observations to made at high sensitivities. Only one instrument was operational in prime mode at a time, but the camera was used in parallel mode to acquire extra astronomical data whenever it was possible. The long-wavelength channel of the photometer was used during satellite slews, this produced a partial sky survey, which covers ~15 % of the sky, at wavelengths around 200 μm. After launch, a parallel/serendipity mode was added for the LWS, in which narrow-band data were obtained at 10 fixed wavelengths in parallel with the main instrument and also during slews.

New generations of space and air-borne integral field spectrometers required large format arrays of low noise equivalent power (NEP) detectors. NEP is the radiant power that produces a signal-to-noise ratio of unity at the output of a given detector at a given data-signaling rate or modulation frequency, operating wavelength, and effective noise bandwidth. In the FIR, photoconductors still offer the higher sensitivity under low background conditions in combination with moderately low operation temperatures (1.7 K to 4 K) when compared to bolometers. In the 40 to 200 μm range, Gallium-doped germanium (Ge:Ga) photoconductors are commonly used because of their high sensitivity. Ge:Ga photoconductors which are mechanically stressed are used to cover the wavelength range from 115 to 210 μm. Unstressed Ge:Ga detectors are used to cover the wavelength range from 40 to 115 μm.

The ISO Camera instrument consisted of two optical channels, used one at a time, each with a 32 x 32 element detector array, operated in the wavelength ranges 2.5-5.5μm and 4-17μm.

The ISOPHOT instrument consisted of three subsystems: ISOPHOT-C, ISOPHOT-P and ISOPHOT-S:

ISOPHOT-C consists of two photometric far-infrared cameras, used one at a time, for the wavelength range 50-240μm. The `C100' camera contained a 3x3 array of Ge:Ga detectors, each with a pixel field of view of 43.5", and 6 filters covering wavelengths up to 105μm. The `C200' camera used a 2x2 array of stressed Ge:Ga detectors with a pixel field of view of 89" and had 5 filters covering wavelengths longwards of 100μm.

ISOPHOT-P was a multi-band, multi-aperture photo-polarimeter for the wavelength range 3-110μm. It contained 13 apertures ranging in size from 5" to 180" and 14 different filters. ISOPHOT-S was a dual grating spectrophotometer which provided a resolving power of ~90 in two wavelength bands simultaneously (2.5-5μm and 6-12μm).

The ISO Long Wavelength Spectrometer covered the wavelength range 43-196.7μm with a spectral resolving power of ~200. Using also the Fabry-Pérot (FP) etalons, the resolution could be increased to around 10,000.

The ISO Short Wavelengths Spectrometer covered the wavelength range 2.38-45.2μm with a spectral resolving power of the order of 1000-2500. Using also the Fabry-Pérot (FP) etalons, the resolution could be increased to more than 25 000 for the wavelength range 11.4-44.5μm.

ISO was operated in a pre-planned manner without any significant routine real-time interaction. ~45% of the observing time was reserved for guaranteed time programmes. But as an observatory, ESO was open to the astronomical community including expert and non-expert users.

Each of the four instruments had a number of possible operating modes. To simplify the definition of an observation and to allow users to specify their observation in terms familiar to them, a set of astronomically-useful operating modes was defined and presented to users as a set of `Astronomical Observation Templates' (AOTs). Each AOT was designed to carry out a specific type of astronomical observation.

~65% of ISO's observing time was distributed to the general community via the traditional method of proposals and peer review. The scientific programme for ISO consisted of more than 1 000 individual proposals.. About 10% of ISO's time was used for Solar System studies, 23% for the Interstellar Medium (ISM), 29% on Stellar/Circumstellar topics, 27% for Extragalactic observations and 11% for Cosmology.

2.4.1.2 Most important results

ISO has delivered important results in nearly all fields of astronomical research. Nearly 1400 papers have been published in the refereed literature on ISO results. A few example from ISO's most important scientific results:

- the discovery of crystalline silicates outside our own solar system, in the atmospheres of young and old stars and also in comet Hale-Bopp. Figure 7.2 show the ISOCAM image of Hale-Bopp comet at 15 μm. This discovery shows that water is ubiquitous in the cosmos.

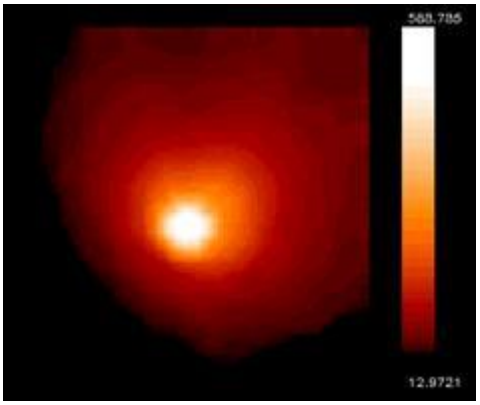

Figure 7.2: ISOCAM image of comet Hale-Bopp at 15 μm (http://iso.esac.esa.int/galleries/sso/halebopp.html, Credit: ESA/ISO, ISOCAM, R. Walsh, B. Altieri, P. Lamy)

- a wealth of water vapour transitions were measured e.g. in Mars, Titan, the giant planets, comets including Hale-Bopp, in shocks, in the cold interstellar medium, in circumstellar envelopes and in the ultra-luminous galaxy Arp220. The spectral resolution of most water observations was limited, but the possibility to observe the full mid- and far-infrared spectrum has opened great possibilities.
- the first detections of the lowest pure rotational lines of H_2 in young massive stars, HH-objects, the diffuse ISM, outer parts of edge-on galaxies. . Temperatures less than a few hundred K could be investigated.
- observing pre-main sequence stars with SWS and LWS spectrographs. These data were used for line detections and to reconstruct the spectral energy distributions. Figure 7.3 shows the spectral energy distribution of 2 Herbig Ae/Be stars. Very different SEDs were observed for Herbig Ar/Be stars, confirming the fact that these objects do not constitute a homogeneous class.

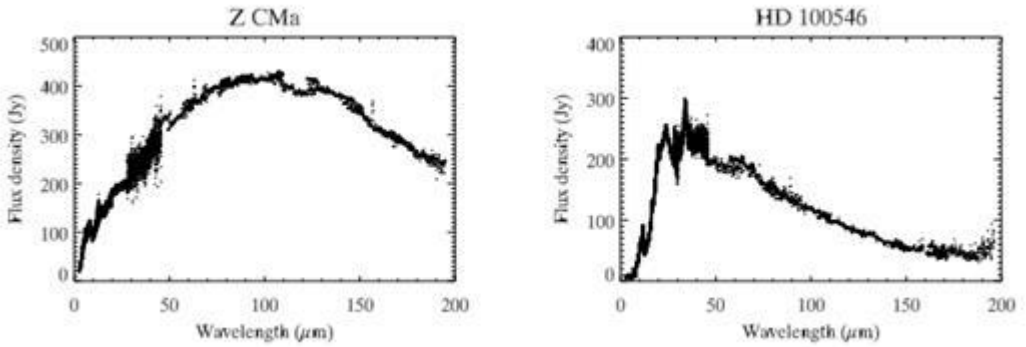

Figure 7.3: *ISO spectra of two Herbig Ae/Be stars (Lorenzetti 2004).*

- detecting planet formation around old, dying stars. E.g. in the vicinity of the Red Rectangle old binary star in the Monoceros constellation, a ring of matter constituting the first stage of planet formation was detected. This discovery contradicted theories that planet formation was only possible around young stars. Figure 7.4 shows two images in red light and the ISO LWS spectrum of the Red Rectangle. The left image was taken by H. van Winckel (Leuven) using the 90 cm Dutch telescope at the European Southern Observatory, La Silla, Chile. The right hand image was taken by G. Weigelt and R. Osterbart (Bonn) using the 2.2m Max Planck telescope, also at E.S.O.. A prominent dark lane is visible across the image, which is due to the disk surrounding the binary system. The tick marks on the spectrum indicate the position of the oxygen-rich olivine bands, suggesting that the disk contains oxygen-rich material. This disk may be the site of on-going planet formation.

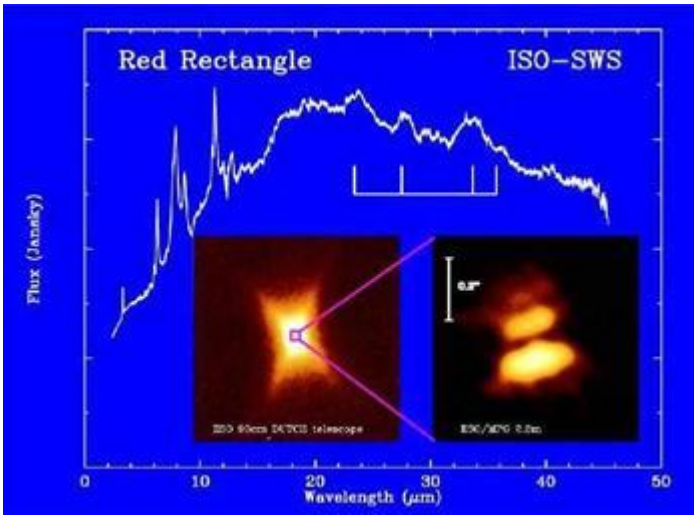

Figure 7.4: *Two images in red light and ISO LWS spectrum of Red Rectangle.(http://coolcosmos.ipac.caltech.edu/image_galleries/ISO/sws/redrec.html)*

- ISO searched for, and found several protoplanetary disks: rings or disks of material around stars which are considered to be the first stage of planet formation.
- the detailed investigations of interstellar solid state features, e.g. CO_2 ices. It gives the possibility to have detailed interplay between observations and laboratory spectroscopy
- obtaining spectral energy distributions of extragalactic objects, which serve as templates for cosmological studies, helped to consolidate the unified scheme or to develop quasar evolutionary scenarios. ISOPHOT SED of NGC6240 are seen on Figure 7.5.

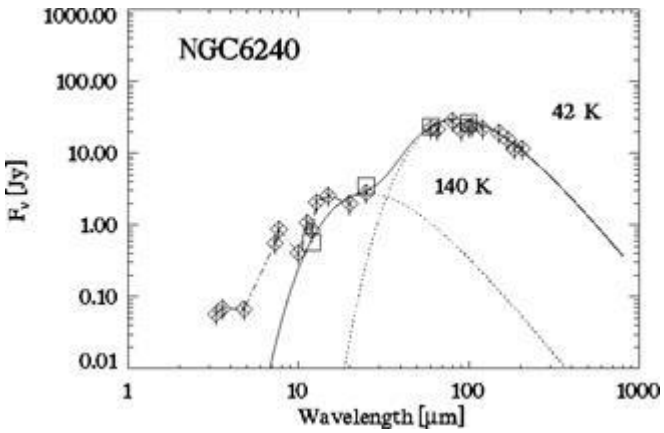

Figure 7.5: ISOPHOT spectral energy distribution of NGC6240. The SED is well fitted with two components: a 140 K and a 42 K blackbody radiation. (http://iso.esac.esa.int/galleries/nor/ngc6240c.htm, Credit: EAS/ISO, ISOPHOT, U. Klaas)

- making deep cosmological surveys at near- and far-infrared wavelengths. It resolved the part of the cosmic infrared background (CIB) into discrete sources and detected fluctuations in the CIB.
- making the European Large Area ISO Survey to explore obscured galaxies and quantify the recent star-formation history of the Universe. This survey discovered 9 hyper luminous galaxies.

3 IAP-IRS Unit Design

3.1 Concept

Candidates:

tbd

4 Realization

5 Test Rig

5.1 Costs

IAP-IRS Parts List

		Cost
		$300
		$100
		$250
		$80
		$200
		$200
		$200
		$50
		$50
		$50
		$20
		$20
		$30
		$30
		$50
		$30
		$50
		$20
		$20
		$20
		$20
		$20
	Total	$1.810

Possibility: Oxygen schneidesystem umbauen

6 Next working packages

7 Suppliers Data

7.1 Electronics, Control

- CNCLab
- قطرنجي للإلكترونيات EKT Beirut
  - Number: 01 820020
  - Website: www.ekt2.com

- Bashir electronics - البشير للإلكترونيات

7.2 Satellite Parts

Specification form © Surrey Satellite Technology Ltd., Tycho House, 20 Stephenson Road, Surrey Research Park, Guildford, Surrey, GU27YE, United Kingdom, Tel: +44(0)1483803803 | **Fax:**+44(0)1483803804 | **Email:** info@sstl.co.uk | **Web:**www.sstl.co.uk

Remark: No answer to email has come.

7.3 CNC Fine Mechanics (2D)

The company HI-TECH Facrication takes CAD Data (in .dxf format) -> Changing to CAM Data.

Satellite Parts are in Alluminium Alloy.

7.4 3D Printing (Plastics)

http://www.cnclablb.com/

7.5 CNC

Company	Phone number	Description	Address	E-mail web site
CNC LAB	06 412 895 03 476 916	Manufacture 3D design in plastic & open source hardware	Tripoli,Lebanon Bahsas,Behind Haykalieh Hospital, Harba Bld.	www.cnclab.com info@cnclablb.com
Hasan Al Baba	03 828 256	Manufacture and casting	Tripoli, Lebanon Mina, Industry and Commerce street	
HI-Tech fabrication Fawaz Abdel Hadi	06 442 787 70 751 522	Precision mechanical parts manufacturing brass & steel marking heads maker	Tripoli, Lebanon Mahjar suhi P.O. Box 1274	www.hitechfabrication.com info@hitechfabrication.com sirfawaz@yahoo.com
Hannuf mechanical 'Corporation for casting and art construction	06 387 723 03 717 107	Manufacture and casting	Tripoli, Lebanon Al Badawi	
GPS Steel	03 196 225	Uses electric discharge machining process to shape any metal material rapidly by using desired modeled electrodes	Beirut, Lebanon Burj Hammoud	Gps.steel.co@gmail.com
Riyako factory	79 118 779	3D CNC machine, manufacture cupboard for cars	Tripoli, Lebanon Badawi, behind Al Ridani bakery	

References

7.6 References and further reading to the 2.6

Beichman, C. A. et al. 1984, *"The formation of solar type stars - IRAS observations of the dark cloud Barnard 5"*, ApJ, 278, 45

Cohen, M., Walker, R. G., Carter, B., Hammersley, P., Kidger, M., Noguchi, K., 1999: *"Spectral Irradiance Calibration in the Infrared. X. A Self-Consistent Radiometric All-Sky Network of Absolutely Calibrated Stellar Spectra"*, AJ, 117, 1864

Cohen, M., Megeath, S. T., Hammersley, P. L., Martin-Luis, F. & Stauffer, J., 2003a: *"Spectral Irradiance Calibration in the Infrared. XIII. ``Supertemplates'' and On-Orbit Calibrators for the SIRTF Infrared Array Camera"*, AJ, 125, 2645

Cohen, M., Wheaton, W. A., Megeath, S. T., 2003b: *"Spectral Irradiance Calibration in the Infrared. XIV. The Absolute Calibration of 2MASS"*, AJ, 126, 1090

Cutri R. M. et al., 2012: *"WISE All-Sky Data Release"*, NASA/IPAC Infrared Science Archive , 2012yCat,2311,0C

Hauser, M. G. et al. 1998: *"The COBE Diffuse Infrared Background Experiment Search for the Cosmic Infrared Background. I. Limits and Detections"*, ApJ, 508, 25

Kataza, H. et al., 2010: ***"****AKARI/IRC All-Sky Survey Point Source Catalogue Version 1.0- Release Note (Rev.1)"*

Kawada, M., Baba, H., Barthel, P.D., et al., 2007: *"The Far-Infrared Surveyor (FIS) for AKARI"*, PASJ, 59, S389

Kim, H.-J. et al. 2012: *„Star Formation in the Long Filamentary Infrared Dark Cloud at l ∼ 53°.2"*, Proceedings of the International Astronomical Union, Symposium 292, Volume 8, pp 46

Kim, H.-J. et al. 2013: *„Star Formation Activity in the Long Filamentary Infrared Dark Cloud IRDC G53.2"*, poster at Protostars and Planets VI, Heidelberg, July 15-20, 2013, http://www.mpia-hd.mpg.de/homes/ppvi/posters/1S015.pdf

Müller, T. G., & Legerros, J. S. V., 1998: *"Asteroids as far-infrared photometric standards for ISOPHOT"*, A&A, 338, 340

Müller, T. G.; Lagerros, J. S. V., 2002: *"Asteroids as calibration standards in the thermal infrared for space observatories"*, A&A, 381, 324

Murakami, H., Baba, H., Barthel, P. et al., 2007: *"The Infrared Astronomical Mission AKARI"*, PASJ, 59, S369

Nakagawa, T. et al. 2007: *"Flight Performance of the AKARI Cryogenic System"* PASJ, 59, 377

Neugebauer, G. et al. "*Early Results from the Infrared Astronomical Satellite"*, (http://www.sciencemag.org/content/224/4644/14.long)

Planck Collaboration, 2011: *"Planck early results. I. The Planck mission"*, A&A, 536, A1

Schlegel, D. J., Finkbeiner, D.P., & Davis, M., 1998: *"Maps of Dust Infrared Emission for Use in Estimation of Reddening and Cosmic Microwave Background Radiation Foregrounds"*, ApJ, 500, 525

Schulz, B., et al. 2002: *"ISOPHOT - Photometric calibration of point sources"*, A&A, 381, 1110

Simon, R., et al., 2006: *"A Catalog of Midcourse Space Experiment Infrared Dark Cloud Candidates"*,ApJ, 639, 227

Wright, E.L., Eisenhardt, P.R.M., Mainzer, A.K. et al., 2010: *"The Wide-field Infrared Survey Explorer (WISE): Mission Description and Initial On-orbit Performance"*, AJ, 140, 1868

Yamamura, I., Makiuti, S., Ikeda, N. et al., 2010, *"AKARI/FIS All-Sky Survey Point Source Catalogues"*, 2010yCat,2298,0Y

http://astron.berkeley.edu/davis/dust/index.html

http://irsa.ipac.caltech.edu/Missions/msx.html

http://lambda.gsfc.nasa.gov/product/cobe/